

Dynamic Model of Cable-Conduit Actuation for Interaction with Non-Passive Environments

Andrew Borowski, Alexander Metz, Fabrizio Sergi, *Member, IEEE*

Abstract—Remote actuation is useful in human-interacting robots to reduce dynamic loading on distal joints. Cable-conduit transmissions, sometimes referred to as Bowden cable or tendon-sheath actuation, are a lightweight option for transferring power to a distal joint from a remotely located actuator. However, the nature of such transmissions causes the system to suffer from diminished efficiency and high reflected impedance as a result of distributed frictional effects between cable and conduit. A dynamic model is useful to produce controllers capable of accurately tracking force or displacement at the system’s output.

In this paper, we present a new computational model for cable-conduit systems that describes interaction with non-passive environments. Unlike previous models, our model features bi-directional propagation of motion within the cable-conduit system. This allows for simulation of human-interacting systems where both the human and the robot have the capability to impose motion or force. Because of this feature, the developed model is applicable to a wide range of physical systems. The model is validated in a physical prototype through experiments involving physical interaction with a human subject. We show that our model accurately predicts behaviors observed in the experimental system.

I. INTRODUCTION

Human-interacting robots frequently employ remote actuation to transmit power to actuated joints. As opposed to co-located actuation, remote actuation permits roboticists to optimize actuator placement such that their placement minimally affects the natural dynamics and energetics of the limb being manipulated [1].

Cable-conduit transmissions, which employ a fixed outer sheath and mobile inner cable, are a common choice for remote actuation due to their flexibility, low mass, and ability to withstand large forces. However, the nested cable design introduces non-negligible frictional losses and mechanical compliance. Consequently, the transmission suffers from diminished mechanical efficiency and backlash, leading to input-dependent stability properties [2]. As an additional consequence, the large damping introduced by friction in turn increases the reflected impedance of the system. While careful design decisions may limit friction, these effects remain significant enough that the system exhibits poor tracking performance without proper compensation.

We gratefully acknowledge the support of the National Science Foundation via grant no. 1638007, and from the University of Delaware Research Foundation.

A.B. and F.S. are with the Human Robotics Laboratory, Department of Biomedical Engineering, and with the Department of Mechanical Engineering, University of Delaware, Newark, DE 19713.

A.M. is with the Human Robotics Laboratory, Department of Biomedical Engineering, University of Delaware, Newark, DE 19713.

Corresponding author (F. S.): (fabs@udel.edu)

Many existing human-interacting robots utilizing cable-conduit transmissions employ only a single cable, allowing the cable to be slacked when the desired torque is zero [3], [4], [5]. However, single-cable systems can only apply torque in one direction. While systems that use two cables have bidirectional torque transfer capabilities, these systems also require more careful control since slacking both cables to achieve zero torque is impossible, and use cable tension [6] or axial torque [7], [8] sensors for feedback.

Numerous specialized feedback laws for frictional effects present in cable conduit systems have been studied. Townsend et al. [9] considered basic schemes, such as integral control and feed-forward Coulomb friction compensation, but found that the presence of stiction caused convergence to a limit cycle rather than the desired value. Several more recent efforts [10], [11], [12] have developed nonlinear compensation laws for use in real-time feedback control. These provide significant performance improvements, but are based on simplified models, which assume a constant cable configuration or interaction with a passive environment. Using a more general model in a feedback

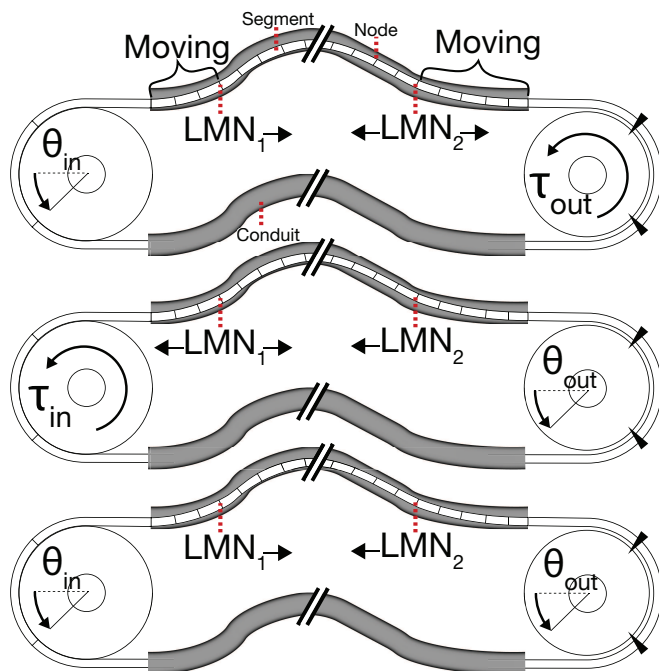


Fig. 1. Schematic diagram of the proposed cable-conduit actuation model, featuring all 3 operating modes (Position-Torque, Torque-Position, Position-Position). Note the model’s ability to change the number of mobile cable segments at both ends of the conduit, as appropriate.

controller could allow for improved system performance in applications involving human-robot interaction.

The first dynamic models of the cable-conduit transmission were developed by Kaneko et al. [2], [13]. Taking a lumped-mass approach, these early models approximated the inner cable as a series of interconnected mass-spring-damper systems. This provided reasonably accurate estimations of system behavior, but was constrained to constant curvature, pretension and environment stiffness. This lumped-mass model was later improved upon by Palli & Melchiorri [14] who used the dynamic Dahl friction model. Do et al. [10], [15], [16] further improved the accuracy of friction estimation by studying a wide array of models and selecting a modified Bouc-Wen model. However, restrictions imposed by a lumped-mass formulation limit the range of physical systems to which these models apply.

Instead of using a lumped-mass approach, Agrawal et al. [17], [18] discretized a set of partial differential equations in cable displacement and tension for arbitrary pretension and curvature. Their new formulation allowed for the study of multiple cable systems, and reproduces the phenomenon of partial movement within the cable, where one regions of the cable moves while the remainder remains stationary. Their derivation, however, constrained the model to the study of systems that interact with passive environments and are position-controlled at their input. These limitations are highly restrictive for the study of practical systems. Typical input actuators, such as DC motors, are torque regulated, not position regulated. Additionally, assuming interaction with a passive environment imposes that motion can only propagate in a single direction in the cable. Fig. 1 shows that when considering active environments motion will need to propagate in both directions. Since human-robot interaction focuses on the interaction with active environments, models of cable-conduit transmissions for human-robot interaction must not assume monodirectional motion propagation.

This paper expands upon the model of Agrawal et al. [17], [18] by developing a modified set of equations that solve for the complete state of the cable-conduit system in the presence of any two applied tensions or displacements, as shown in Fig. 1. As such, the model is capable of propagating motion from either side of the cable, in both directions, concurrently, to describe the interaction with non-passive environments.

II. TRANSMISSION MODEL

A. Theory

We develop our model based on the assumption of an axially linear elastic cable. We present our innovations and the crucial aspects of the model formulation here; the full derivation of the base formulation can be found in [18].

Since the governing differential equations for the system are unsolvable in practice, we instead choose a finite-element approach. The cable is divided into a number of discrete segments, over each of which system parameters such as radius of curvature are approximated as constant. The number of segments presents a trade-off between numerical accuracy and computational complexity.

A given segment i of cable experiences frictional losses in tension due to contact between cable and sheath. Tension T_i creates a normal force between cable and conduit at a given point as a function of the radius of curvature $R(i)$, given by $F_n \approx T_i R(i)^{-1} dx$. Normal force F_n is assumed to be constant over the given segment's length Δx . This can be multiplied by coefficient of friction, as a function of segment velocity v_i , and direction of motion, $\mu(v_i)$ and S_i respectively, then integrated along the cable. The result is a change in tension between the two ends of the cable segment $T_{i,i+1}$ defined as:

$$\frac{T_{i+1}}{T_i} = \exp\left(\frac{\mu(v_i)S_i\Delta x}{R(i)}\right) \quad (1)$$

Additionally, since the cable is modeled as an elastic element with spring constant K_c , Hooke's Law provides a relationship between the change in tension across a segment due to friction and the change in length of the segment,

$$u_{i+1} - u_i - \frac{R(i)S_iT_i}{K_c\mu(v_i)} \left(\exp\left(\frac{\mu(v_i)\Delta x S_i}{R(i)}\right) - 1 \right) = 0 \quad (2)$$

where u_i and T_i represent the displacement of and tension at the i th node. These two equations fully define the state of all moving segments in the cable, and are evaluated at each timestep during simulation for segments $i = 1$ to $k - 1$. If instead a node is stationary, its tension and position cannot change from one iteration to the next. When a stationary node n is adjacent to the "last moving node" (LMN) k , a boundary condition for the motion of the mobile segment(s) of cable is given by

$$u_k + \frac{T_k\Delta x}{2K_c} = u_n - \frac{T_n\Delta x}{2K_c} \quad (3)$$

The equations above yield $2k - 1$ equations while in partial motion, or $2k - 2$ equations during mass motion, but there are $2k$ free variables (k each of position, tension) defining the cable state. To solve the system, at least two additional constraint equations are required. These equations specify either the exact value of a variable (e.g. a known input position, or measured tension), or relate two variables in a way not linearly dependent with existing equations (e.g. an equation representing a position-tension relationship of a spring environment). Furthermore, two modeled cables can be connected to a load pulley in a pull-pull configuration by including appropriate constraints on their end positions.

Motion propagates through the cable when the first stationary node n on the cable becomes the new LMN, k . This condition is verified when the difference in cable tension at that node can overcome static friction,

$$T_n S_k \geq T_k S_k \exp\left(\frac{\mu(v_i)\Delta x}{R(n)}\right) \quad (4)$$

A change in LMN means that an additional segment would have moved during the previous time instant, and requires its re-evaluation. The LMNs reset to the first and last node of the cable when motion stops or changes direction, since every segment will be required to overcome stiction at these instants. Lastly, in the event that a cable becomes slack,

(i.e. it has non-positive tension), our model neglects any contributions from this cable until it is no longer slack.

B. Friction Modeling

Previous models using this formulation relied on simple Coulomb friction. Our model specifies the friction coefficient μ for a given segment i as a function of that segment's velocity, v_i , calculated at the previous timestep as

$$v_i = (\dot{u}_i + \dot{u}_{i+1})/2 \quad (5)$$

For the sake of comparison with prior works, we elect a simple stiction model

$$\mu(v_i) := \begin{cases} \mu_s & \dot{v}_i = 0 \\ \mu_d & \dot{v}_i \neq 0 \end{cases} \quad (6)$$

throughout all experiments presented except where otherwise specified.

C. Variable Inputs/Outputs

Previous models treated u_1 as an input and required the existence of $f(x)$ such that $u_{N+1} = f(T_{N+1})$, where N is the number of cable segments being simulated. We relax this constraint by allowing any couple of the set $\{u_1, u_{N+1}, T_1, T_{N+1}\}$ to be specified as input. If the input couple specifies at least one position variable, the system is fully defined. Otherwise, the system of (1,2) requires an additional world-frame displacement law (e.g. a bulk mass) to calculate absolute positions instead of relative ones. As such, we exclude the couple $\{T_1, T_{N+1}\}$ for purposes of this paper.

Allowing arbitrary variables to be specified removes the previous assumption that the environment is passive. As a result, the model cannot assume motion will always propagate from the proximal end of the cable to the distal end. To accommodate this, the model introduces the possibility of a second last moving node, k_2 , which can propagate from the distal-most node of the cable back toward the proximal end. When k and k_2 do not coincide, each end of the cable is treated as a separate system and solved independently, since no motion or tension can be transmitted through non-moving nodes. When the two moving nodes k and k_2 coincide, the cable begins to move *en masse* and is solved as a single system.

III. MODEL VALIDATION

A. Experimental Apparatus

A test platform was designed to include a cable-conduit transmission between a DC motor and a handle constrained to apply torques along the flexion/extension axis of a human wrist. In this scenario, the human would apply effort to accomplish motion and the remote actuator would be controlled so as to display desired force/torque at the point of interaction to display virtual dynamic environments.

Fig. 2 shows a schematic of the test bed. The cable mounting plates can slide to facilitate pretensioning of the system. The system has a fixed transmission ratio R of approximately 5, specified by the ratio of radii between the

load and motor pulleys. Torque is supplied by a DC motor (Maxon motors 355679). Torque from the motor is measured via current sensing. For static tests, the load pulley can be locked to its support structure by a bolt such that the applied torque can be measured by the 6 channel force/torque sensor (ATI mini40, resolution 0.5 mNm, 4 Nm at full-scale output). Position can be measured at both ends via encoders present at both the actuator (2000 cpt) and load shaft (10000 cpt). When a human is present, an additional passive degree of freedom at the handle compensates for any misalignment between the anatomical and robotic flexion/extension axes.

Each cable consists of a 2 m wound steel wire sheath with HDPE liner with an approximate inner diameter of 1.75 mm (Lexco Cable 408187), and an inner cable with a 7x19 stranded stainless steel core coated in nylon to a final outer diameter of 0.75 mm (Sava Cable 210149). The cables are arranged in a typical pull-pull configuration used to allow for bidirectional transmission of motion and force.

B. Parameter Estimation

The model has eight free parameters describing the mechanical properties of the system. Cable length, curvature radius, and both pulley radii were measured directly. The elastic coefficient of the inner cable was estimated by a measurement of the stretch-vs-force relationship for both cables in parallel with output pulley blocked. Pretension is calibrated using a spring stretched to prescribed lengths to move the cable mounts. The friction coefficients were

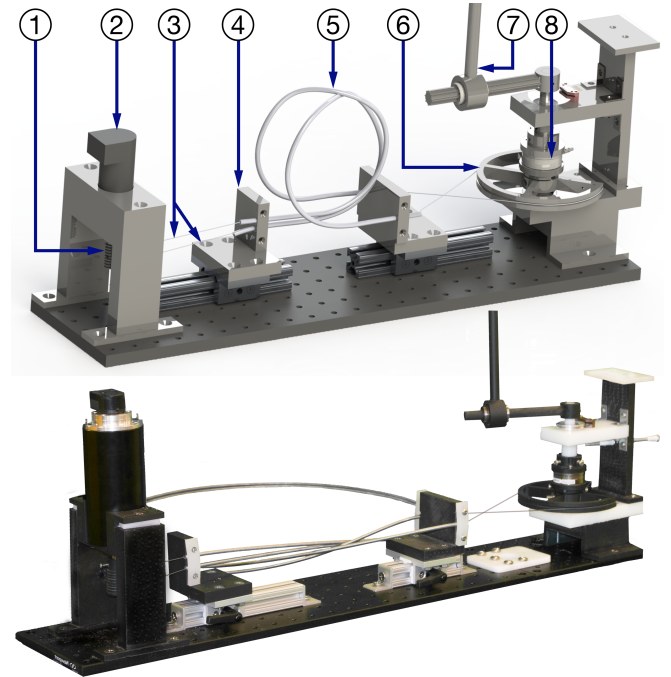


Fig. 2. Top: Rendering of test apparatus design. The system is comprised of an input motor (2) and its pulley (1), which drives two steel inner cables (3) through their conduits (5), causing motion of the load pulley (6) and therefore the handle for human interface (7). Mobile conduit supports (4) pretension the cable, and load torque is measured by loadcell (8). Bottom: Photograph of the constructed system.

estimated by minimizing the difference between model and physical results during an experiment similar to those described in the following subsection, but this trial was not used for any comparisons. Table I lists the values provided to the model for each experiment, unless otherwise specified.

TABLE I
SYSTEM PARAMETERS USED FOR MODEL SIMULATION

L	$R(x)$	r_{input}	r_{load}	K	T_0	μ_d	μ_s
2 m	0.28 m	20 mm	104 mm	$2 \frac{\text{kN}}{\text{m}}$	10 N	0.21	0.63

C. Experiment 1: Behavioral Verification

In Experiment 1, we aimed to check that the model reacts correctly to changes in relevant physical parameters such as cable pre-tension and radius of curvature. To do so, the load pulley was locked, and the motor applied a torque alternatively ramping up and down with a slope of ± 0.1 Nm/s to a maximum of ± 0.125 Nm then dwelling for 0.5 s before reversing direction.

Under this paradigm, we first studied variations in pretension (Experiment 1a). Pretension in the cables was set to 4 levels by using a spring stretched to different lengths to adjust the position of one cable mounting plate. The motor then applied its prescribed torque profile for 30s. The model was given the prescribed motor torque profile and fixed load

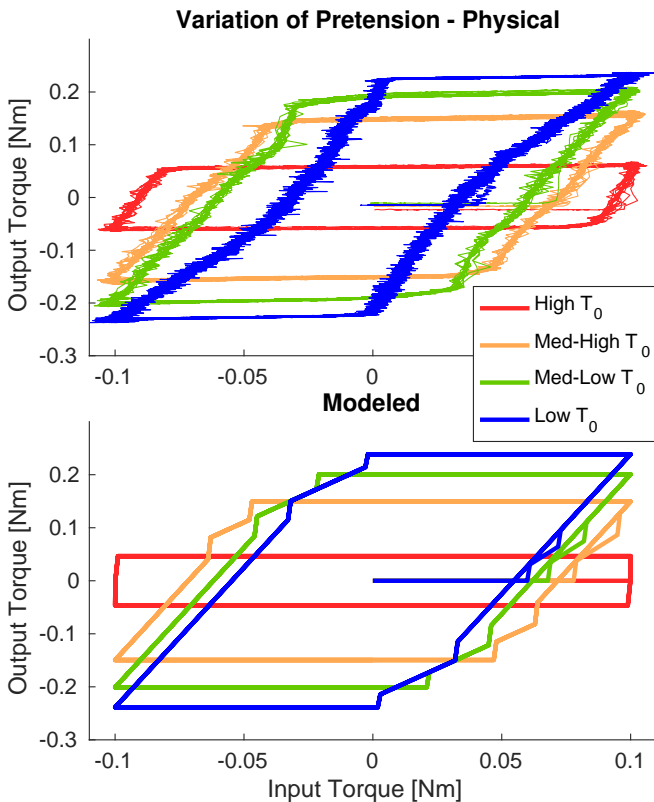


Fig. 3. Exp. 1a: Physical system and modeled behavior when pretension in the cables is varied. The model reproduces the trends in behavior introduced by variations in pretension correctly.

angle as inputs. Only the pretension variable was changed in the model between trials. The results of this experiment are visible in Fig. 3. In agreement with eq. (1), increased pretension causes increased friction, decreasing efficiency. This effect is visible both in the experiment and the model.

The experiment was repeated with the cable forced into a path consisting of 1, 2, or 3 loops (Experiment 1b). The ability to describe correctly the transmission dynamics under changing configuration is of critical importance to wearable robotic applications, where the cable's path is usually time varying. For this condition, pretension was fixed at a constant level set before each trial to ensure consistency. As visible in Fig. 4, increased cable curvature results in larger backless and decreased transmission efficiency, both in simulation and experiment.

D. Experiment 2: Position-Force Mode

In Experiment 2, we validated our model's capability of capturing dynamic interaction with an active environment. Here, the motor is controlled to apply a torque τ (expressed in newton-meters) in response to the angular displacement θ (in radians), given by

$$\tau(\theta) := \begin{cases} \min(-\frac{1}{2}(\theta + 0.05), 0.2) & \theta < -0.05 \\ 0 & |\theta| \leq 0.05 \\ \max(-\frac{1}{2}(\theta - 0.05), -0.2) & \theta > 0.05 \end{cases} \quad (7)$$

During the experiment, the participant was instructed to move the handle periodically, imposing an amplitude of at

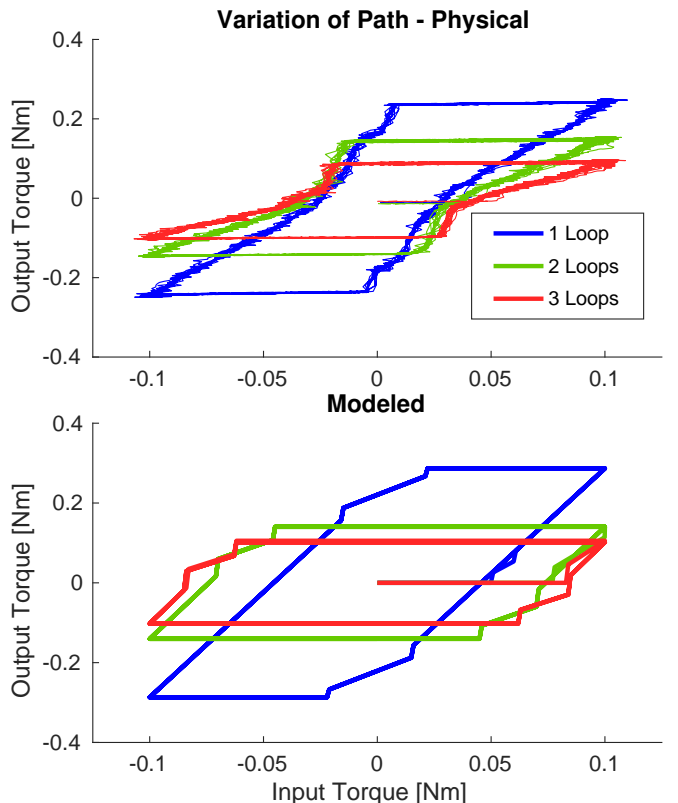


Fig. 4. Exp. 1b: Variations in system behavior when cable path is changed.

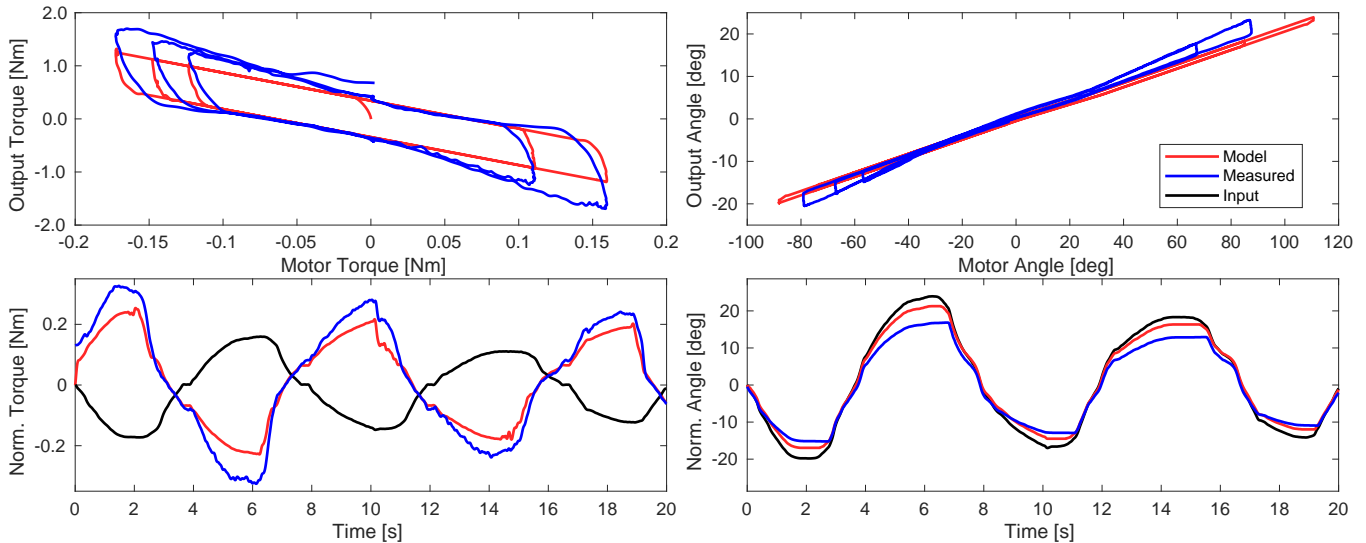


Fig. 5. Exp. 2: Simulated and physical error-reduction tunnel behavior. Torques and pulley angles have been scaled by the transmission ratio R in the lower plots.

least 40 deg. The trajectory imposed by the human and the corresponding requested motor torque were then input to the model which repeated the experiment in simulation. Model parameters were left unchanged from Experiment 1. Fig. 5 presents position and torque relationships both in the experiment and simulation. Results show a qualitative match between experiments and simulations. Fig. 6 shows the hysteresis present in rendering of this virtual dynamic environment imposed by the transmission, both as captured by the experiment and simulation.

There exists a numerical discrepancy between the model and physical results. Some of this error can be attributed to shortcomings of the over-simplified stiction model used. We analyzed the behavior of the model in presence of a viscous friction term, and verified that the residuals (sum of squares of difference in torque values between simulated and experimental data) are reduced by about 50% (Fig. 7). It is

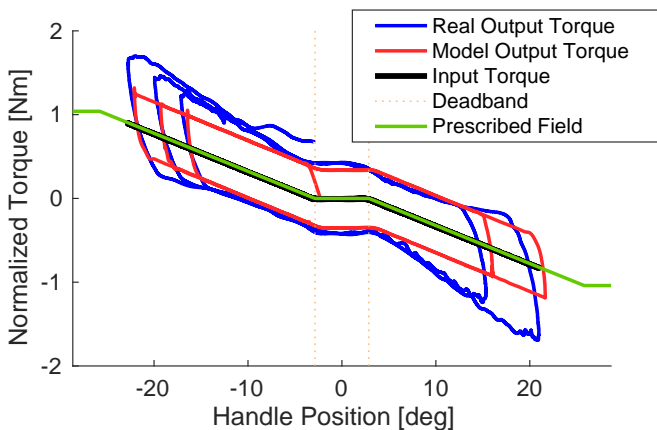


Fig. 6. Exp. 2: A comparison of the prescribed error-reduction tunnel and the measured torque when implemented naively with remote actuation. Accurate prediction of this behavior will allow for compensation of the effect.

expected that the use of a more advanced model will further reduce the residuals.

E. Experiment 3: Position-Position Mode

Our third experiment aimed to validate the capability of our model in the position-position case. For a high-friction transmission, intuition suggests that when input and output impose identical trajectories, each source is responsible for moving one half of the cable, requiring compensation of 50% of the system's friction. For this experiment, the human applied a periodic trajectory to the load pulley while the motor was controlled with a stiff PI position controller with desired angle $\theta_{des} = R\theta_{load}$. We expect that the non-ideality of this position controller will distort the anticipated sharing of effort and lead to asymmetry in the measured torques.

Two methods were used to replicate this experiment in the model. Both methods specified the load-side trajectory as one input. In the first, the model is given a motor trajectory specified by $\theta_{motor} = R\theta_{load}$, representing the

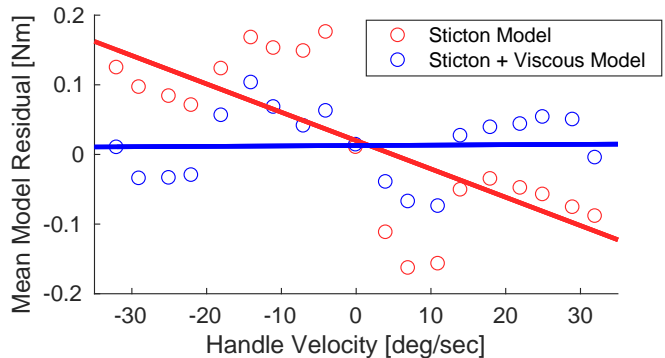


Fig. 7. Exp. 2: Comparison between modal residuals, and their linear fits to velocity, with and without inclusion of a viscous friction term. Decreases in residual from improving the friction model suggests using a specialized friction model such as in [16] could improve accuracy of modeled results.

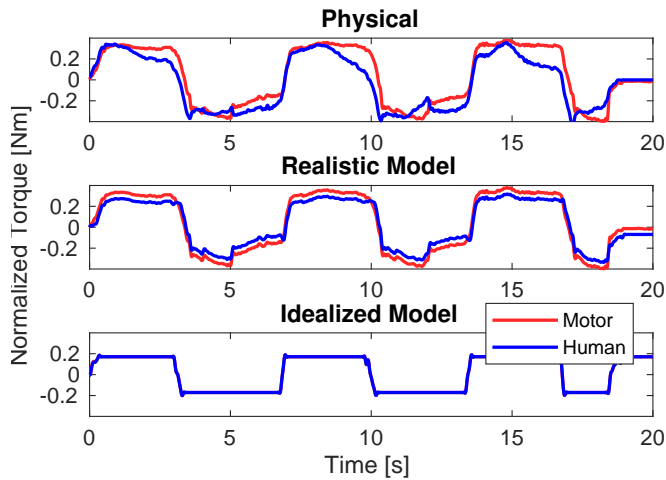


Fig. 8. Exp. 3: A comparison of physical, realistically modeled, and ideally modeled position-follower systems. Using measured torque as input for dynamic system (Realistic Model) reproduces some of the asymmetry seen in the experiment.

ideal, infinitely stiff position controller. In the second, the model applies the same torque at the motor as the real PI controller applied, as to simulate the behavior of the non-ideal controller used in the experiment.

Fig. 8 shows that under the ideal conditions, torques at both motor and load match the expected behavior of perfectly splitting the effort needed to overcome friction. The results from the experiment and second simulation demonstrate similar asymmetries in load sharing resulting from the non-ideal nature of the position controller.

IV. CONCLUSION

We have developed and validated a novel cable-conduit transmission model capable of describing interaction of robots with active environments. The simulated results of our model match qualitatively effects observed in experiments conducted with a benchtop cable-conduit transmission prototype involving non-passive human interaction.

Since some of the numerical discrepancy can be attributed to the simplified friction model, we expect that including friction models specifically designed for cable-conduit transmissions [16] will allow for more accurate predictions of engagement behavior as well as capture trends resulting from other unmodeled frictional effects. Furthermore, allowing for variable-length segments as a function of their instantaneous radius of curvature will allow for optimization of the computational complexity of the model. This will be of benefit for wearable applications, where regions of large curvature are usually only near human joints.

Future work involves integrating this model and available sensor technologies into a state estimator to be used in real-time control applications, and developing new sensing techniques to further take advantage of the computational capabilities now available.

REFERENCES

- [1] R. C. Browning, J. R. Modica, R. Kram, and A. Goswami, "The effects of adding mass to the legs on the energetics and biomechanics of walking," *Medicine and Science in Sports and Exercise*, vol. 39, no. 3, pp. 515–525, 2007.
- [2] M. Kaneko, W. Paetsch, and H. Tolle, "Input-dependent stability of joint torque control of tendon-driven robot hands," *IEEE Transactions on Industrial Electronics*, vol. 39, no. 2, pp. 96–104, apr 1992.
- [3] A. T. Asbeck, R. J. Dyer, A. F. Larusson, and C. J. Walsh, "Biologically-inspired soft exosuit," in *IEEE International Conference on Rehabilitation Robotics*. IEEE, jun 2013, pp. 1–8.
- [4] J. Zhang, C. C. Cheah, and S. H. Collins, "Experimental comparison of torque control methods on an ankle exoskeleton during human walking," in *2015 IEEE International Conference on Robotics and Automation (ICRA)*. IEEE, may 2015, pp. 5584–5589.
- [5] K. Heer, J. Lee, N. Collins, M. Auger, and O. Celik, "Design and Control of a Modular Lower-Limb Exoskeleton Emulator for Accelerated Design and Evaluation of Assistive Gait Exoskeleton Parameters," in *Proceedings of the 41st Annual Meeting of the American Society of Biomechanics*, 2017, pp. 475–476.
- [6] J. F. Veneman, R. Ekkelenkamp, R. Kruidhof, F. C. T. Van Der Helm, and H. Van Der Kooij, "Design of a series-elastic and bowdencable-based actuation system for use as torque-actuator in exoskeleton-type training," in *Proceedings of the 2005 IEEE 9th International Conference on Rehabilitation Robotics*, vol. 2005. IEEE, 2005, pp. 496–499.
- [7] F. Sergi, A. Erwin, B. Cera, and M. K. O'Malley, "Compliant force-feedback actuation for accurate robot-mediated sensorimotor interaction protocols during fMRI," *5th IEEE RAS/EMBS International Conference on Biomedical Robotics and Biomechanics*, pp. 1057–1062, aug 2014.
- [8] A. Schiele, P. Letier, R. Van Der Linde, and F. Van Der Helm, "Bowden cable actuator for force-feedback exoskeletons," *IEEE International Conference on Intelligent Robots and Systems*, pp. 3599–3604, 2006.
- [9] W. Townsend and J. Salisbury, J., "The Effect of coulomb friction and stiction on force control," *Proceedings. 1987 IEEE International Conference on Robotics and Automation*, vol. 4, pp. 883–889, 1987.
- [10] T. N. Do, T. Tjahjowidodo, M. W. S. Lau, and S. J. Phee, "Position control of asymmetric nonlinearities for a cable-conduit mechanism," *IEEE Transactions on Automation Science and Engineering*, vol. PP, no. 99, pp. 1515–1523, jul 2015.
- [11] Q. Wu, X. Wang, L. Chen, and F. Du, "Transmission Model and Compensation Control of Double-Tendon-Sheath Actuation System," *IEEE Transactions on Industrial Electronics*, vol. 62, no. 3, pp. 1599–1609, mar 2015.
- [12] Y. Jung and J. Bae, "Torque control of a double tendon-sheath actuation mechanism in varying sheath configuration," in *2017 IEEE International Conference on Advanced Intelligent Mechatronics (AIM)*. IEEE, jul 2017, pp. 1352–1356.
- [13] M. Kaneko, M. Wada, H. Maekawa, and K. Tanie, "A new consideration on tendon-tension control system of robot hands," *1991 IEEE International Conference on Robotics and Automation (ICRA)*, no. April, pp. 1028–1033, 1991.
- [14] G. Palli and C. Melchiorri, "Model and control of tendon-sheath transmission systems," in *Proceedings - IEEE International Conference on Robotics and Automation*, vol. 2006. IEEE, 2006, pp. 988–993.
- [15] T. N. Do, T. Tjahjowidodo, M. W. S. Lau, and S. J. Phee, "Dynamic Friction-Based Force Feedback for Tendon-Sheath Mechanism in NOTES System," *International Journal of Computer and Electrical Engineering*, vol. 6, no. 3, pp. 252–258, 2014.
- [16] T. N. Do, T. Tjahjowidodo, M. W. Lau, and S. J. Phee, "A new approach of friction model for tendon-sheath actuated surgical systems: Nonlinear modelling and parameter identification," *Mechanism and Machine Theory*, vol. 85, pp. 14–24, 2015.
- [17] V. Agrawal, W. J. Peine, and Bin Yao, "Modeling of a closed loop cable-conduit transmission system," in *2008 IEEE International Conference on Robotics and Automation*. IEEE, may 2008, pp. 3407–3412.
- [18] V. Agrawal, W. J. Peine, and B. Yao, "Modeling of Transmission Characteristics Across a Cable-Conduit System," *IEEE Transactions on Robotics*, vol. 26, no. 5, pp. 914–924, oct 2010.